RESEARCH ARTICLE



Unraveling mechanisms of selenium recovery by facultative anaerobic bacterium *Azospira* sp. A9D-23B in distinct reactor configurations

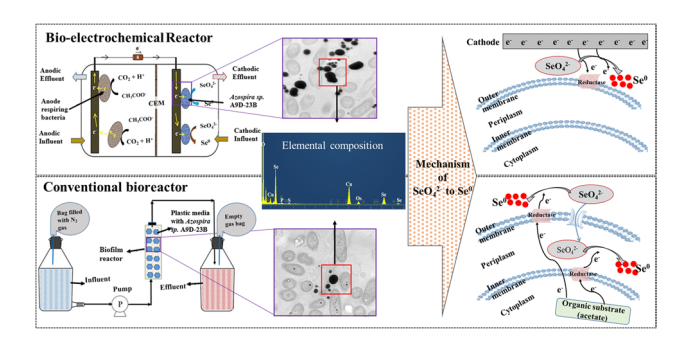
Benhur Kessete Asefaw¹ · Nidhi Walia^{2,3} · Margaret Elizabeth Stroupe^{2,3} · Huan Chen⁴ · Youneng Tang¹

Received: 2 May 2024 / Accepted: 21 September 2024 © The Author(s), under exclusive licence to Springer-Verlag GmbH Germany, part of Springer Nature 2024

Abstract

Microbial processes are crucial in the redox transformations of toxic selenium oxyanions. This study focused on isolating an efficient selenate-reducing strain, Azospira sp. A9D-23B, and evaluating its capability to recover extracellular selenium nanoparticles (SeNPs) from selenium-laden wastewater in different reactor setups. Analysis using transmission electron microscopy (TEM) and energy-dispersive X-ray spectroscopy (EDX) revealed significantly higher extracellular SeNPs production (99%) on the biocathode of the bioelectrochemical (BEC) reactor compared to the conventional bioreactor (65%). Further investigations into the selenate reductase activity of strain A9D-23B revealed distinct mechanisms of selenate reduction in BEC and conventional bioreactor settings. Notably, selenate reductases associated with the outer membrane and periplasm displayed higher activity (18.31 ± 3.8 μ mol/mg-min) on the BEC reactor's biocathode compared to the upflow anaerobic conventional bioreactor (3.24 ± 2.9 μ mol/mg-min). Conversely, the selenate reductases associated with the inner membrane and cytoplasm exhibited lower activity (5.82 ± 2.2 μ mol/mg-min) on the BEC reactor's biocathode compared to the conventional bioreactor (9.18 ± 1.6 μ mol/mg-min). However, the comparable kinetic parameter (Km) across cellular fractions in both reactors suggest that SeNP localization was influenced by enzyme activity rather than selenate affinity. Overall, the mechanism involved in selenate reduction to SeNPs and the strain's efficiency in detoxifying selenate below levels regulated by the U.S. Environmental Protection Agency has broad implications for sustainable environmental remediation strategies.

Graphical Abstract



Keywords Biocathode \cdot *Azospira species* \cdot Selenate \cdot Se redox \cdot Selenium nanoparticles \cdot Enzyme activity \cdot Electron microscope

Responsible Editor: Gerald Thouand

Published online: 27 September 2024

Extended author information available on the last page of the article

Introduction

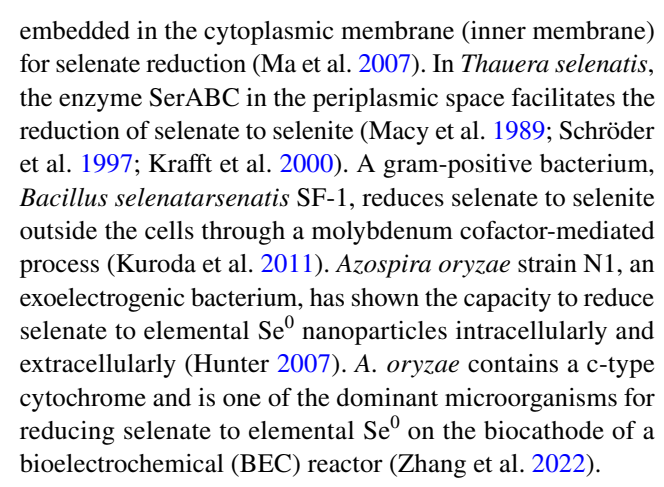
Selenium, a trace element that occurs naturally in mineralbased fuels, shale, and alkaline soils (Haygarth 1994; Ridley et al. 2006), plays a dual role as an essential mineral for animals and humans and as a toxin when consumed in



excessive doses (Stadtman 1996; Rayman 2002; Watts et al. 2003). Anthropogenic activities such as mining, agricultural, industrial operations, and petrochemical processes are primary contributors to selenium contamination (from 0.4 µg/L to 4.9 mg/L) in the environment (Pearce et al. 2009; Tang et al. 2015; Gingerich et al. 2018; Tan et al. 2018a; Zhang et al. 2020; Holmes et al. 2023). The maximum allowable concentration of total selenium in drinking water has been set at 50 µg/L by the United States Environmental Protection Agency (USEPA 2015) and in the effluent of industrial wastewater at 76 µg/L (USEPA 2019). Exceeding selenium concentration limits can lead to health problems, including reproductive failure, congenital disabilities, and hair loss (Losi and Frankenberger 1997; Hatfield et al. 2014). The dominant selenium formed in the contaminated water are oxyanions, including selenate (SeO₄²⁻) and selenite (SeO₃²⁻). However, selenium may also exist as elemental Se⁰ and selenide (Se²⁻).

Numerous researchers have endeavored to recuperate Se⁰ nanoparticles that were synthesized within biological reactors (Macy et al. 1993b; Soda et al. 2011; Zhang et al. 2018a; Lai et al. 2020), as their retrieval could offset treatment expenses, given selenium's widespread utilization in diverse industrial applications like semiconductors and alloys (Nancharaiah and Lens 2015; Staicu et al. 2015). Selenium is one of the critical elements in low-carbon energy technologies (Moss et al. 2011; Liang and Gadd 2017) and is identified as a high-risk element susceptible to supply and other constraints (Graedel et al. 2015). A hurdle to effective Se⁰ nanoparticle recovery is that conventional bioreactors produce predominantly intracellular Se⁰ nanoparticles regardless of the bacteria used (Zhang et al. 2018b, 2022). While the extraction of extracellular Se⁰ nanoparticles from biomass for recovery can be achieved through techniques like centrifugation or selective adsorption, the recovery of intracellular Se⁰ nanoparticles presents more challenging barriers, necessitating an additional step of cell lysis, which is resource-intensive and involves the utilization of chemicals (Shakibaie et al. 2010; Sonkusre et al. 2014; Tang and Chen 2019).

The process of selenate reduction has been studied in various bacteria through biochemical and genetic analyses. Different bacterial species employ specific mechanisms for this reduction. For instance, *Citrobacter freundii* and some other facultative anaerobic bacteria utilize genes expressing the YnFE enzyme to reduce selenate to elemental Se⁰ on the outer membrane and in the periplasm (Theisen and Yee 2014). Similar mechanisms have been observed in *Escherichia coli* and *Salmonella enterica*, where the YnfE enzyme catalyzes selenate reduction outside the cytoplasm (Guymer et al. 2009). The enzyme SerT from the aerobic bacterium *Comamonas testosteroni* S44 facilitated selenite reduction within the periplasm (Tan et al. 2018b). Alternatively, *Enterobacter cloacae* SLD1a-1 employs the TatC enzyme



Studies showed that the BEC and conventional bioreactors inoculated with the same mixed cultures reduce selenate differently, mainly extracellular reduction in the BEC reactor versus intracellular reduction in the conventional bioreactor (Zhang et al. 2022). Despite the evidence from STEM images regarding the localization of elemental Se⁰ produced in those distinct reactors, the molecular mechanisms of selenate reduction in these bioreactors remain elusive. Hence, in this study, a facultative anaerobe selenate-reducing bacteria was isolated from the cathode effluent of the BEC reactor. This isolate was characterized for potential application in removing selenate from industrial wastewater and recovering elemental Se⁰ for the nanotechnology sector. Thus, the main aim of this study is to understand the molecular mechanisms underlying the differences observed in the localization of elemental Se⁰ produced. This will involve investigating the strain's selenate reductase performance in both reactors using the isolated pure culture. Understanding the sophisticated mechanism of selenate reduction to elemental Se⁰ and the strain's efficiency in detoxifying selenate below the USEPA levels has broad implications for leveraging microbial processes for sustainable environmental remediation strategies.

Materials and methods

Pure culture isolation

A liquid sub-sample (~3 mL) from the cathode chamber effluent of the BEC reactor (Zhang et al. 2022) was incubated in a crimp-sealed bottle containing 100 mL of growth medium, devoid of agar, with nitrogen gas in the headspace. The bacteria used in Zhang et al. (2022) was brought from a wastewater treatment plant located in Tallahassee, Florida. Cells were collected by centrifugation and washed with deionized water. One milliliter of the diluted cell suspension was gently mixed with 25 mL of soft agar supplemented by sodium acetate (CH₃COONa, 40 mM) and sodium selenate



(Na₂SeO₄, 10 mM) in each Petri dish and incubated at 30 °C. The content of the growth medium and agar media is provided in supplementary data. After 3–4 days, single red-colored colonies, indicative of selenate reduction, were transferred into separate crimp-sealed bottles filled with an anaerobic growth medium (30 mL) supplemented with sodium nitrate (NaNO₃, 10 mM) as the electron acceptor. Using nitrate instead of selenate helped minimize elemental Se⁰ nanoparticles interfering with the following experiments.

After 5 days, 3 mL of the growth phase liquid samples was transferred to other crimp-sealed bottles with growth media, and sodium selenate was added to one of the bottles as an electron acceptor to verify the culture's selenate reduction capability. A red hue observed after 72 h confirmed the culture's ability to reduce selenate to elemental Se⁰. The pure culture was subjected to polymerase chain reaction (PCR) amplification and phylogenetic assay described below.

PCR amplification and phylogenetic assay

For the 16S rRNA gene analysis, the genomic DNA was extracted from the pellet of a 500 µL overnight culture using E.Z.N.A. Bacterial DNA Kit (OMEGA BIO-TEK) followed by PCR amplification with universal primers 27F and 1492R. Nucleotide sequencing was performed using the Sanger dideoxy sequencing method in the cloning and sequencing facility at Florida State University (Florida, USA). The Molecular Evolutionary Genetics Analysis (MEGA 11) software assembled the forward and reverse sequences (Tamura et al. 2021). Database searches and nucleotide sequence alignment were conducted using the Basic Local Alignment Search Tool (BLAST) provided by the National Center for Biotechnology Information (NCBI). The 16S rRNA partial sequence of the pure culture was deposited into Genbank under the accession number OQ983537. A neighbor-joining tree (Saitou and Nei 1987) was constructed using MEGA 11 (Tamura et al. 2021), and the sequences were retrieved from the BLAST database. Bootstrap values were computed in MEGA 11, following the approach outlined by Felsenstein (1985). Evolutionary distances were calculated using the Maximum Composite Likelihood method, as described by Tamura et al. (2004).

Reactor setup and operation

A BEC reactor (Fig. S1) and a conventional biofilm reactor (Fig. S2) were established in an anaerobic chamber at 30 °C, as previously described by Zhang et al. (2022). The cathode electrode (carbon cloth) of the BEC reactor and plastic media of the conventional bioreactor were incubated for 14 days with the pure culture prior to reactor utilization. Nevertheless, the anode electrode of the BEC reactor was incubated with an activated sludge sourced from a local

wastewater treatment plant. The membrane pieces ($0.1 \mu m$ pore diameter, Nuclepore track-etched membranes, Whatman, USA) placed at the bottom of the BEC compartments collected precipitates for subsequent analysis. The conventional bioreactor consisted of a column filled with plastic media (BioFLO 9, Smoky Mountain Bio Media) designed for biofilm attachment.

Post incubation, the carbon cloth and the plastic media were transferred to the cathode chamber of the BEC reactor and the conventional bioreactor, respectively. Graphite carbon cloth electrodes (3 cm×5 cm, Fuel cell Store, USA) were used in the anode and cathode chambers, remaining completely submerged during the experimental period. The electrodes were connected to a 100 Ω external resistor with a copper wire throughout the experiment. The anode chamber was provided with a medium (Zhang et al. 2018b) supplemented with sodium acetate (CH₃COONa, 34.2 mg/L) as the sole electron donor, while the cathode chamber received a similar medium with sodium selenate (Na₂SeO₄, 11.4 mg/L) as the electron acceptor. This synthetic media is used to simulate the wastewater in our study. The supply rate of the media used in the conventional reactor control was kept the same as the BEC reactor at 330 mg Se/m²-day. The ratio of carbon to selenium fed to the reactors was 2:1, higher than the stoichiometric ratio of 0.4:1 (see reaction below) to ensure that carbon was not limiting.

$$0.125 CH_3COO^- + 0.093SeO_4^{2-} + 0.19 H^+ + 0.022NH_4^+$$

= 0.022 $C_5H_7O_2N + 0.093Se + 0.037 HCO_3^-$
+ 0.037 $CO_2 + 0.193 H_2O$

Sampling and chemical analysis

Samples (influent and effluent) were collected weekly from both chambers of the BEC reactor and the conventional bioreactor for chemical analysis. Selenium species (dissolved selenate (SeO_4^{2-}) and selenite (SeO_3^{2-}), solid Se^0 in effluent, and solid Se⁰ in the reactor) and other dissolved species, including acetate and sulfate, were analyzed. Ion chromatography (IC, Dionex Aquion Ion Chromatography System, USA) was used to measure SeO₄²⁻ and SeO₃²⁻ in the influent and effluent. The effluent solid Se⁰ was determined by subtracting the total soluble selenium from the total selenium measured in the effluent sample using a microwave plasma-atomic emission spectrometer (4100 MP-AES, Agilent Technologies, USA). To obtain the total soluble selenium, the sample was first filtered through a syringe filter (pore size 20 nm) and then centrifuged at 21,000 xg for 0.5 h. The difference between total solid selenium and effluent solid selenium is the total solid selenium in the reactor. The total solid selenium was computed by subtracting the



soluble selenium in the effluent from the influent selenate. Sulfate reduction and acetate oxidation were continuously monitored by measuring them using ion chromatography. The presence of dissolved sulfide (S^{2-}) after $SO_4^{\ 2-}$ reduction was measured using a UV–Vis spectrophotometer (UV-2501 PC, Shimadzu, USA), with the absorbance recorded at 664 \pm 10 nm. Gas chromatography (GC, model SRI 8610C, SRI instruments, USA) was used to measure methane production in the reactors' headspace. After purging with pure nitrogen gas, the dissolved oxygen concentration in the influent media was kept below 0.2 mg/L. The influent media's pH was kept at ~7.0, and the effluent sample's pH was 7.2 ± 0.2 .

Solid samples were collected during steady-state from bioanode, biocathode, and retentate collected from the cathode effluent after being filtered with a membrane filter and from the plastic media in the column of the conventional reactor for further characterization. Transmission Electron Microscopy (TEM, Hitachi HT7800, USA) coupled with EDX was used for elemental analysis. Before taking images, the samples were pretreated and coated with osmium to prevent thermal damage and enhance image contrast. Details of sample preparation and pretreatment for TEM imaging were provided in our previous work (Zhang et al. 2022).

Enzyme assay and its activity for selenate reduction

To further determine the activity of the pure culture in continuously operated reactors, cells from each reactor were harvested and centrifuged for 10 min at $10,000 \times \text{g}$ to collect the pellets. The collected pellets were transferred to separate crimp-sealed

vials (30 mL total volume after growth medium addition) and cultured anaerobically at 30 °C for 48 h in a sterile mineral salts medium (Schröder et al. 1997) containing yeast extract (~4 g/L), NaCl (1.2 g/L), Tryptic soy broth (10 g/L), selenate (10 mM), and acetate (10 mM). Due to the necessity for a higher cell concentration for enzyme assay and purification, the 30 mL cultures were further grown into 1000 mL batch cultures. After 48 h, these cultures were harvested at final optical density $(OD_{600} > 0.6)$ by centrifuging cultures for 10 min at $16,000 \times g$ at 4 °C. The cells were cooled at 0 °C and rinsed twice with 10 mM Tris/HCl, pH 8. The cell pellets were resuspended in a sucrose-Tris buffer and subjected to lysozyme and EDTA treatment, following the protocol outlined by Osborn and Munson (1974), to disrupt the cell walls. The suspension was stirred for 15 min on ice and subsequently incubated at 37 °C for 10 min to facilitate the formation of spheroplasts. The removal of spheroplasts was achieved by centrifugation at 25,000×g for 25 min, separating soluble proteins containing the outer and periplasmic enzymes. Further disruption of the spheroplast was carried out using a Sonicator (Branson sonifier 250, USA) with 4 cycles of sonication at 15 s per cycle, ensuring maximum yield of the inner and cytoplasmic enzymes. Post-sonication, the suspension underwent centrifugation at 15,000 x g for 10 min, and the supernatant, containing over 90% of the inner and cytoplasmic purified enzyme, was carefully transferred to a sterile Falcon tube. The purified selenate reductases were subsequently concentrated and stored for activity assays.

After separating the enzymes associated with the outer membrane and periplasm (*i.e.*, the outer and periplasmic enzymes) from the enzymes associated with the inner membrane and

Fig. 1 Neighbor-joining phylogenetic tree illustrating the connection between the isolated selenate-reducing strain (A9D-23B), its nearest relatives, and recently reported selenate-reducing bacteria. Note: Numbers at nodes indicate bootstrap values (1000 replicates). The scale bar represents the number of base substitutions per site

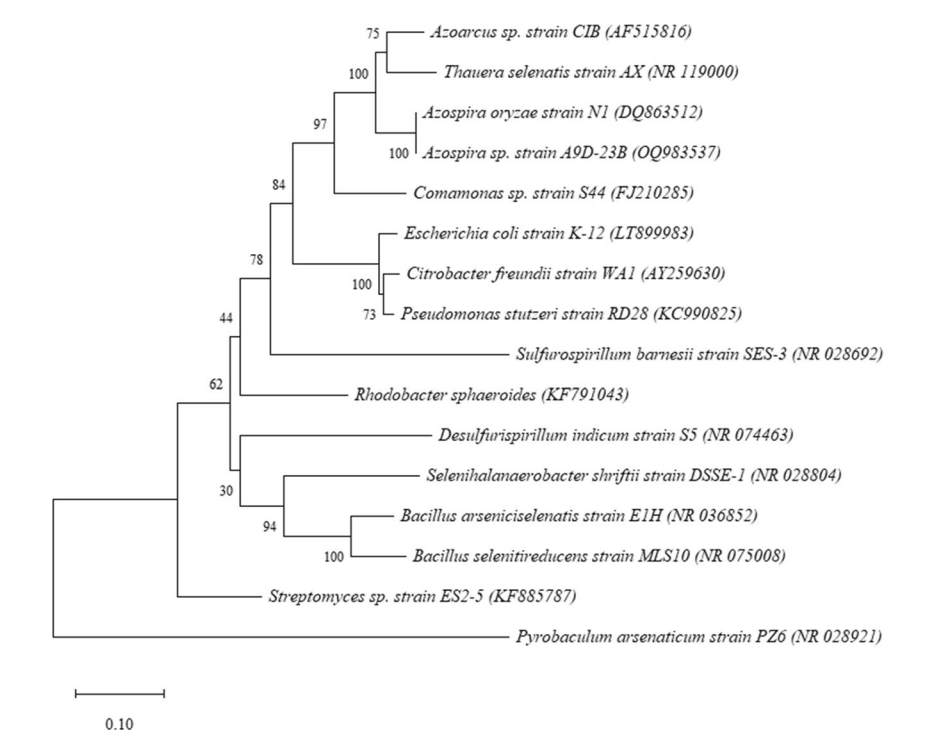
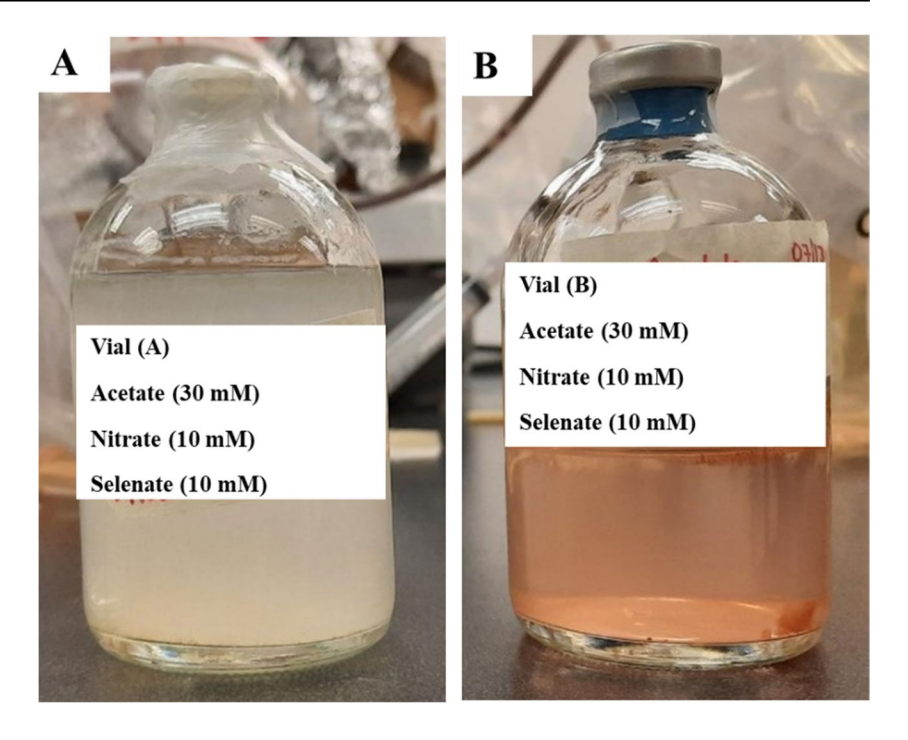




Fig. 2 Azospira sp. A9D-23B pure cultures with acetate and multiple electron acceptors (NO₃⁻, and SeO₄²⁻) in aerobic condition (**A**) and anaerobic condition (**B**). (Note: the reduction of selenate to elemental Se. ⁰ gives vial (**B**) red color)



cytoplasm (i.e., the inner and cytoplasmic enzymes), the protein concentration in each of the two fractions was measured in triplicate ± standard deviation (SD) using the Bovine Serum Albumin (BSA) method. Benzyl viologen, an artificial electron donor, was first reduced using small sodium dithionite aliquots forming a dark violet color in a 50 mM buffer, potassium phosphate, pH 7.4. In place of the cellular electron donor, NADPH, dithionite was selected as a reducing agent because it can reduce the flavins without binding to the protein (Murray et al. 2021). The purified enzyme used an electron donor, the reduced benzyl viologen, to reduce selenate in an anaerobic cuvette. UV-Vis spectrophotometer (Agilent 8453 UV-Vis, USA) was used to measure the oxidized and dithionite-reduced spectrum of the enzyme in anaerobic cuvettes (Lafontaine and Lancaster 2015). The enzyme activity for selenate reduction was determined using the Beer equation (Eq. 1) after recording the absorbance (A₅₅₀) at 550 nm using the spectrophotometer in triplicates \pm SD. Values for $k_{\rm m}$ and $V_{\rm max}$ were the average of the three replicate values \pm SD obtained through the linearized Hans Woolf equation (Eq. 2). The enzyme activity assay is provided in supplementary data.

$$V_0 = \frac{\Delta A}{\varepsilon l} \tag{1}$$

$$\frac{[S]}{V_0} = \frac{[S]}{V_{\text{max}}} + \frac{k_{\text{m}}[S]}{V_{\text{max}}[S]}$$
 (2)

 ΔA : change in absorbance at specific wavelength; l: path length (cm) = 1 cm; V_0 : activity rate of the enzyme in mol/L-min; ε : molar extinction coefficient/absorbance of benzyl

viologen at 550 nm = 8.665 L/mmol-min (Vazquez et al. 2008). It quantifies the extent to which a chemical species or substance absorbs light at a specific wavelength. [S]: concentration of selenate (μ M); $k_{\rm m}$: enzyme affinity to its substrate (μ M); $V_{\rm max}$: maximum velocity (rate of reaction) where the enzyme gets saturated with the substrate (μ mol/min-mg).

Results and discussions

Phylogenetic analysis of strain Azospira A9D-23B

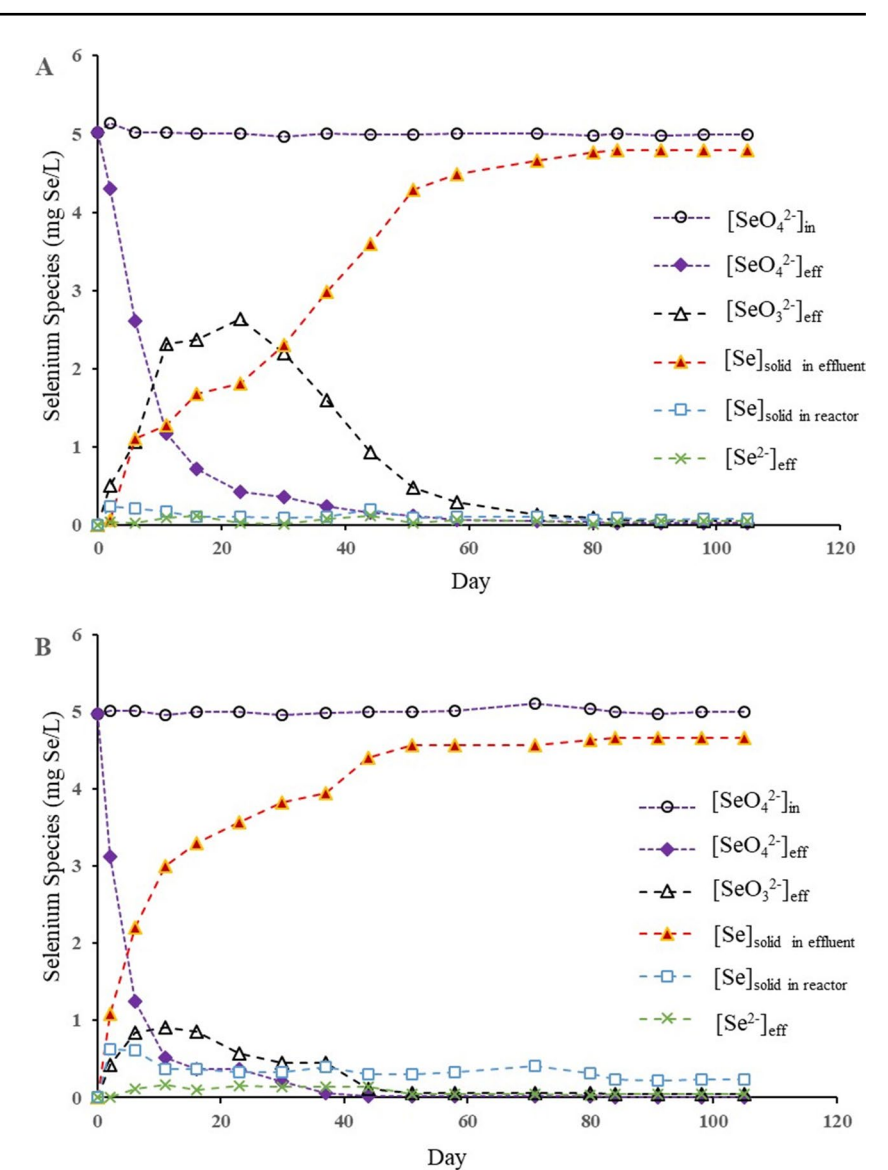
The evolutionary analysis revealed that strain A9D-23B is associated with the *Azospira* genus within the Rhodocy-claceae family of the Betaproteobacteria class, as depicted in Fig. 1. Notably, this strain is the second known bacterium within the *Azospira* genus capable of reducing selenate to SeNPs. Among the well-studied selenate-reducing bacteria, we find representatives from the following genera: *Thauera* (Macy et al. 1993a), *Stenotrophomonas* (Lampis et al. 2017), *Enterobacter* (Ma et al. 2007), *Bacillus* (Kashiwa et al. 2000), *Sulfurosprillium* (Oremland et al. 1999), and *Pseudomonas* (Macy et al. 1989). Interestingly, the closest known relative to strain A9D-23B is *Azospira oryzae* strain N1, originally isolated from a selenate-reducing bioreactor (Hunter 2007). These strains share 99.3% 16S rRNA sequence similarity.

Removal of selenate and elemental Se⁰ production

The selenate reduction ability of the isolated pure culture, *Azospira* sp. A9D-23B, differed significantly depending on



Fig. 3 Selenate reduction in the cathodic chamber of BEC (A) and conventional bioreactor (B)



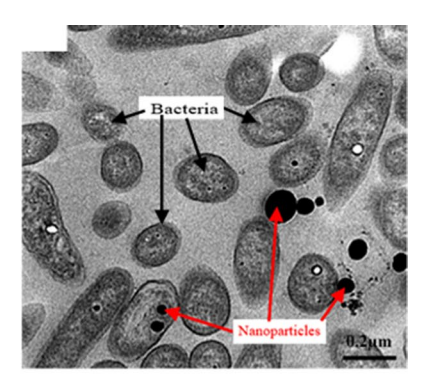
the environmental conditions, despite the consistent dosage of acetate (30 mM) and electron acceptors (NO₃⁻, and SeO₄²⁻) at 10 mM (Fig. 2). Strain A9D-23B showed > 99% similarity with A. oryzae sp., a rod-shaped, gram-negative bacteria known for its ability to reduce SeO₄²⁻ and SeO₃²⁻ to elemental Se⁰. Vial A remained open, and Vial B was sealed with a N₂-CO₂ (4:1) mixture in the headspace. Despite the cloudy appearance indicating bacterial growth in Vial A, no red Se⁰ nanoparticles were observed. Conversely, in Vial B, the culture utilized electrons from acetate to reduce selenate, producing red Se⁰ nanoparticles (Fig. 2). The use of an anaerobic condition in Vial B suppressed the electron flow to oxygen reduction and resulted in the enhancement of selenate reduction to elemental Se⁰. This demonstrated the strain's selenate reduction ability under anaerobic conditions. The cultures were subsequently transferred to the BEC and conventional bioreactors to be tested under the continuous-flow condition.

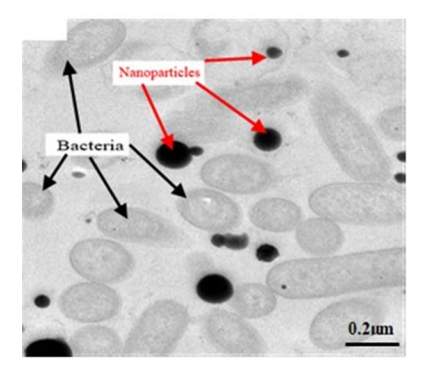
In both reactors, selenate reduction began on the subsequent day of operation and reached below 20 µg Se/L (detection limit) at the steady state (Fig. 3). Initially, selenite, the intermediate species of selenium, accumulated in the first 20 days but diminished (~50 µg Se/L) at the steady state. In both reactors, over 98% of the $SeO_4^{\ 2-}$ was converted to particulate Se⁰, with total dissolved selenium (SeO₄²⁻, SeO₃²⁻, and Se^{2-}) in the effluent of both reactors below 70 μg Se/L, which is the industrial wastewater standard set by USEPA (2019). The initial days of the experiment witnessed a swifter reduction of selenate to elemental Se⁰ in the conventional bioreactor compared to BEC. This discrepancy arose due to the fact that in BEC, the reduction of selenate depended on the transfer of electrons from the anodic chamber to the cathodic chamber through the external circuit and subsequently to the bacteria on the biocathode. This intricate process took a considerable amount of time to stabilize, as elucidated in a previous study



Nanoparticles Bacteria 0.2µm

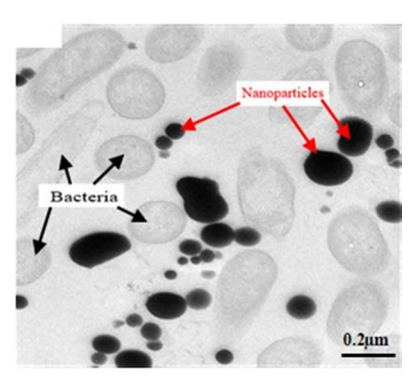
Inoculum

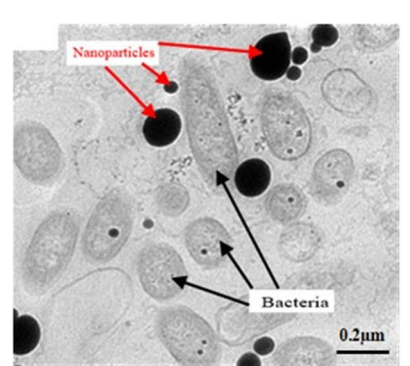




BEC (Left: cathodic effluent,

Right: biocathode)





Conventional bioreactor control

Left: reactor effluent, Right: in the reactor)

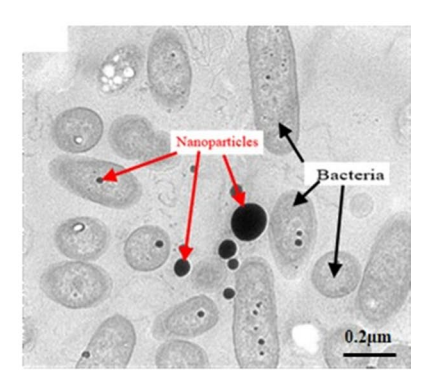


Fig. 4 Representative thin-section TEM images of a mixture of Se⁰ particles and Azospira sp. A9D-23B in the inoculum, BEC, and the conventional bioreactor control

(Zhang et al. 2022). Despite high acetate consumption (94%) in the conventional bioreactor, negligible sulfate reduction activity (~1%) was observed, indicating the culture's primary focus on SeO_4^{2-} reduction (Fig. S3). The amount of S^{2-} detected was also negligible (below the detection limit of the spectrophotometer, <20 µg/L). Only 0.017 mg C/L of CH₄ was produced in the cathode chamber of BEC and conventional bioreactor. This value is insignificant when considering any methanogenesis reduction. The conventional bioreactor served as a control to validate that the biocathode of the BEC reactor, with the same pure culture, produced significantly more extracellular elemental Se^0 than the conventional bioreactor, which is elaborated in the next section.

The substantial flow of electrons from the anode electrode across an external resistor to the biocathode was

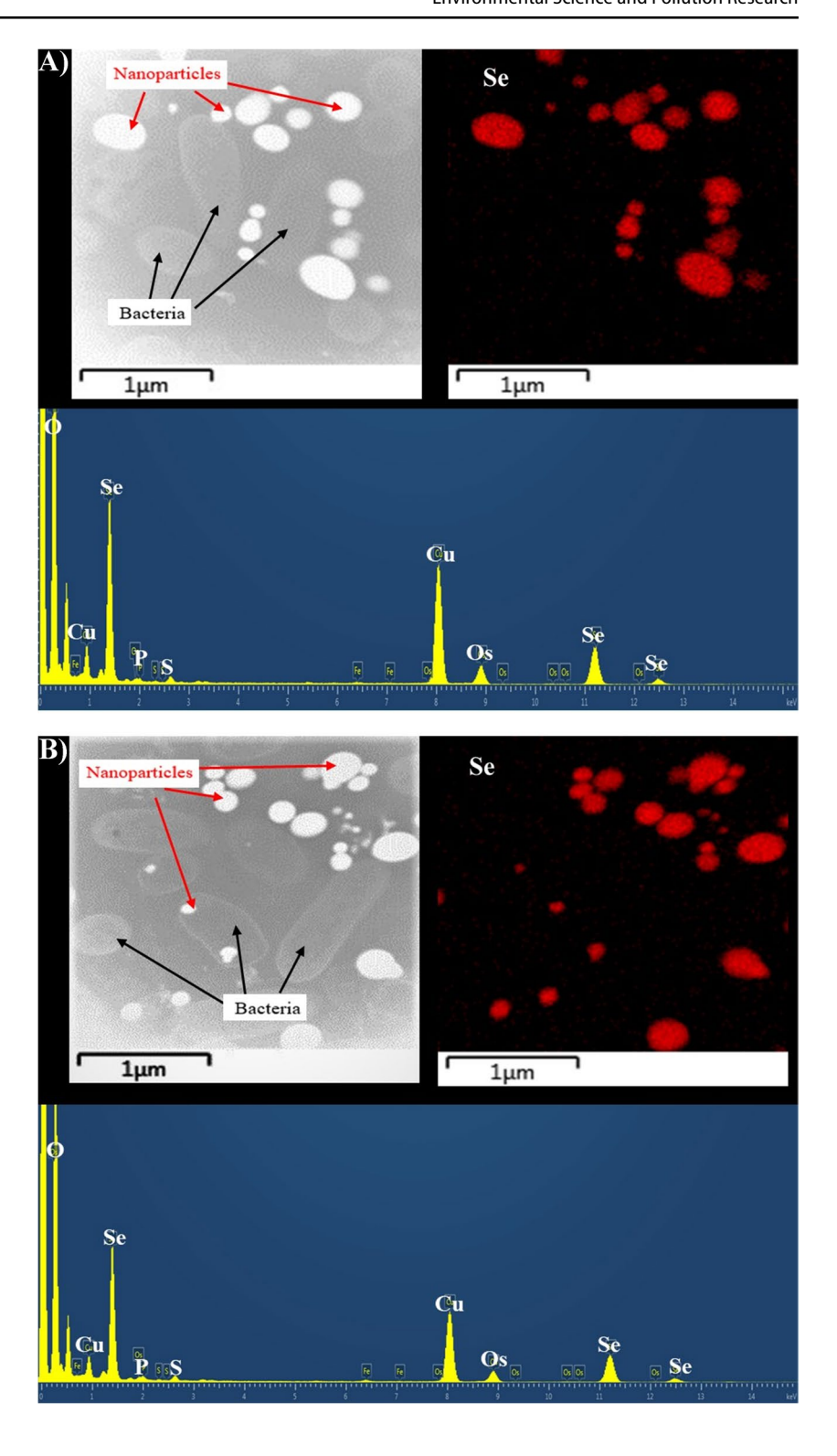
proportional to the selenate reduction rate. Biofilm and other precipitates attached to the membrane surface (CEM) could lead to fouling, decrease membrane permeability, and cause higher internal resistance, impacting the overall performance of the reactor. Periodic membrane cleaning or replacement can reduce the internal resistance of the reactor and maintain the reactor efficiency (Choi et al. 2011).

Characterization of solids in the BEC reactor

Literature reports the microbial reduction of selenate results in the formation of spherical Se⁰ nanoparticles (Stolz and Oremland 1999; Kashiwa et al. 2000; Switzer Blum et al. 2001; Oremland et al. 2004; Yee et al. 2007; Prakash et al. 2009; Kuroda et al. 2011; Lai et al. 2016;



Fig. 5 Representative STEM image accompanied by EDX mapping spectra for Se⁰ particulates: A biocathode of BEC reactor at steady state; B conventional bioreactor control at steady state. Notes: Se⁰ was the predominant element of the nanoparticles; Cu represented the copper grid for holding the samples, and osmium (Os) was used for better image contrast



Zhang et al. 2018b, 2022; Tan et al. 2018b; Nguyen et al. 2019). TEM images corroborated this, showing the accumulation of dense, spherical nanoparticles in both reactors of this study (Fig. 4). Scanning TEM-EDX mapping spectra confirmed the spherical nanoparticles as elemental Se⁰ (Fig. 5), with sizes ranging from 50 to 450 nm. The

L-series signal for Se⁰ was greater than other elements like sulfur (S), phosphorus (P), copper (Cu), and osmium (Os) in the EDX spectra (Fig. 5), indicating high Se⁰ retention within the biofilm matrix. A stark contrast was observed between the BEC and conventional bioreactor regarding Se⁰ nanoparticle accumulation. On the biocathode of the



Table 1 Features of some bacteria cell cultures in the presence of selenate/selenite

Bacteria	Reactor used	% of extracellular Se ⁰ nanoparticles	Size of Se ⁰ nanoparti- cles	References
Azospira sp. A9D-23B	BEC (periplasmic reductase)	~99%	50-200 nm	This study (based on 50 images)
Azospira sp. A9D-23B	Conventional (cytoplasmic reductase)	~65%	50–200 nm	This study (based on 50 images)
Aspergillus niger	Upflow bioreactor	~1%	20-100 nm	Sinharoy and Lens (2022)
Aspergillus niger KP	Airlift bioreactor	<1%	65-100 nm	Negi et al. (2020)
Cronobacter sp. THL1	Bioelectrochemical reactor	~49%	-	Nguyen et al. (2016)
Sulfurospirillum barnesii SES-3	Upflow anaerobic sludge blanket	~81%	200–400 nm	Lenz et al. (2009)
Sulfurospirillum barnesii	Batch experiment	~81%	200–400 nm	Oremland et al. (2004)
Selenihalanaerobacter shriftii	Batch experiment	~86%	200–400 nm	Oremland et al. (2004)
Bacillus selenitireducens	Batch experiment	~90%	200–400 nm	Oremland et al. (2004)
Comamonas testosteroni S44	Batch experiment	~30%	100-300 nm	Xu et al. (2018)
Azoarcus sp. CIB	Batch experiment	~95%	88-160 nm	Fernández-Llamosas et al. (2016)
Stenotrophomonas maltophilia SelTE02	Batch experiment	~96%	160–250 nm	Lampis et al. (2017)
Thauera selenatis	Batch experiment	~1%	150–200 nm	Butler et al. (2012); Debieux et al. (2011)
Rhodopseudomonas palustris N	Batch experiment	~81%	80-200 nm	Li et al. (2014a)
Vibrio natriegens	Batch experiment	~94%	100–400 nm	Fernández-Llamosas et al. (2017)
Rhodospirillum rubrum	Batch experiment	~27%	_	Kessi et al. (1999)
Alcaligenes faecalis Se03	Batch experiment	~96%	250-290 nm	Wang et al. (2018)
Shewanella oneidensis MR-1	Batch experiment	~10%	<100 nm	Li et al. (2014b)
Enterobacter cloacae SLD1a-1	Batch experiment	~99%	<100 nm	Losi and Frankenberger (1997)
Streptomyces sp. ES2-5	Batch experiment	~1%	50-500 nm	Tan et al. (2016)

The percentage of cells having extracellular nanoparticles in most of the previous studies is calculated based on their limited number of TEM images

BEC reactor, less than 1% of the cells contained intracellular Se⁰ nanoparticles, whereas, in the conventional bioreactor, it was ~ 35% (calculated from 50 images).

A comparative analysis of the percentage of extracellular Se⁰ nanoparticles produced between Azospira sp. in BEC and conventional bioreactors versus other bacteria cell cultures in previous studies was performed (Table 1). The production of extracellular Se^0 nanoparticles by Azospira sp. on the biocathode surpassed the figures reported in earlier studies involving other bacterial cultures. While Azospira sp. effectively reduces selenate to elemental Se^0 , the localization of Se⁰ nanoparticles serves as indirect evidence of selenate reductase activity within the cells across different reactors. Direct evidence from selenate reduction assays further supports the identification of active reductase sites within the cells. This led to the hypothesis that the mechanism of selenate reduction to elemental Se⁰ on the biocathode of BEC reactor and in the conventional bioreactor is dependent on the cellular energy cost, selenate transfer pathway, and location of the active selenate reductase. This implied a significant role of proteins associated with the outer membrane and periplasm in the extracellular selenate reduction process, which is further discussed below.

Cellular location of selenate reductase in *Azospira* sp. A9D-23B

Two cell fractions (outer and periplasmic fraction versus inner and cytoplasmic fraction) were separated using the procedure outlined by Osborn and Munson (1974). Selenate reductase activity in these fractions was assayed using an artificial electron donor, benzyl viologen. The reaction started with varying concentrations of selenate (7–1000 μ M), with activity observed by measuring absorbance change at 550 nm within the first 60 s. The purified selenate reductase displayed a peak visible absorbance spectrum at 550 nm when dithionite was used under anaerobic conditions (Fig. S4). However, the air-oxidized spectrum (control) of the selenate reductase did not show any peak at the same wavelength. Despite the variance in enzyme activity for selenate reduction, selenate reductases from cells of



[%] of extracellular Se^0 nanoparticles = $(1 - (number of cells containing spherical <math>Se^0$ particles/total number of cells)) × 100

Table 2 Properties of Azospira sp. A9D-23B selenate reductase from the biocathode of BEC and conventional bioreactor

	Conventional bioreactor	bioreactor				Biocathode, BEC	EC			
	Protein	Total activity	Specific activity K _m	K _m	V _{max}	Protein	Total activity	Total activity Specific activity K _m	K_{m}	V _{max}
	mg/mL	Units/L	Units/mg	μМ	Units/mg	mg/mL	Units/L	Units/mg	Ми	Units/mg
Periplasmic fraction	2.18 ± 0.01 7.08 ± 9	7.08 ± 9	3.24 ± 2.9	118 ± 43	0.014 ± 0.01	7.41 ± 0.01 136 ± 13	136 ± 13	18.31 ± 3.8	114 ± 39	0.09 ± 0.01
Cytoplasmic fraction	10.2 ± 0.01 93.6 ± 9.1	93.6 ± 9.1	9.18 ± 1.6	118 ± 17	0.068 ± 0.00	13.0 ± 0.05	75.9 ± 21	5.82 ± 2.2	164 ± 36	0.04 ± 0.01

Protein concentration is measured using BSA assay; units: µmol/min

the BEC reactor and conventional bioreactor were present in both cell fractions: the outer and periplasmic fraction and the inner and cytoplasmic fraction.

The enzymes from the outer and periplasmic fraction of the biocathode cells in the BEC reactor exhibited the highest specific activity (18.31 \pm 3.8 μ mol/min-mg) shown in Table 2, which was six times the activity observed in the outer and periplasmic fraction from the conventional bioreactor. In contrast, a higher activity of the selenate reductase (9.18 \pm 1.6 μ mol/min-mg) was observed in the inner and cytoplasmic fraction of the conventional bioreactor cells compared to those in the BEC biocathodes (5.82 \pm 2.2 μ mol/min-mg). In both cases, the differences between the activity of selenate reductase are statistically significant ($p \le 0.0002$; see the Supporting Information for details of the statistical analysis).

The location of the selenate reductase, YnfE in Citrobacter freundii (Theisen and Yee 2014) and Escherichia coli K12 and Salmonella enterica serovar Typhimurium LT2 (Guymer et al. 2009), SerABC in Thaeura Selenatis (Krafft et al. 2000), and SrdA in B. selenatarsenatis SF-1 (Kuroda et al. 2011) governed the location of selenate reduction. Similarly, we can conclude that the location of the more active selenate reductase (with high specific activity) in strain A9D-23B determined the location of the produced elemental Se⁰ nanoparticles. For instance, the enzymes in the outer and periplasmic fraction of the biocathode cells exhibited higher specific activity than the inner and cytoplasmic fraction (Table 2), corresponding well to much more extracellular Se⁰ production (99%) on the biocathode. The reason of higher specific activity for the outer and periplasmic enzymes in the BEC cells can be explained by the lower cost of cellular energy for electron and selenate transport to the outer and periplasmic enzymes (Fig. 6). In other words, the extracellular pathway for Se⁰ nanoparticle production had a shorter distance regarding electron transfer and selenate transport compared to the intracellular pathway. Conversely, the higher cellular energy cost for electron transport from the cytoplasm to the outer-membrane reductase deterred substantial extracellular Se⁰ nanoparticle production in the conventional bioreactor (Fig. 6).

This extracellular selenate reduction mechanism on the biocathode protected the bacteria from the toxic intermediate, selenite, as well. In the conventional reactor, despite the higher inner cytoplasmic reductase activity and lower energy cost for electron transport from acetate to inner and cytoplasmic reductases, the bacteria reduced selenate partially outside the cells to avoid selenite toxicity. This led to the reduction of selenate to elemental Se⁰, both intracellularly and extracellularly, in the conventional bioreactor. Nevertheless, the inner membrane-bound selenate reductase in *Azospira* sp. A9D-23B from the conventional bioreactor might play a physiological role in the assimilation of selenium beyond



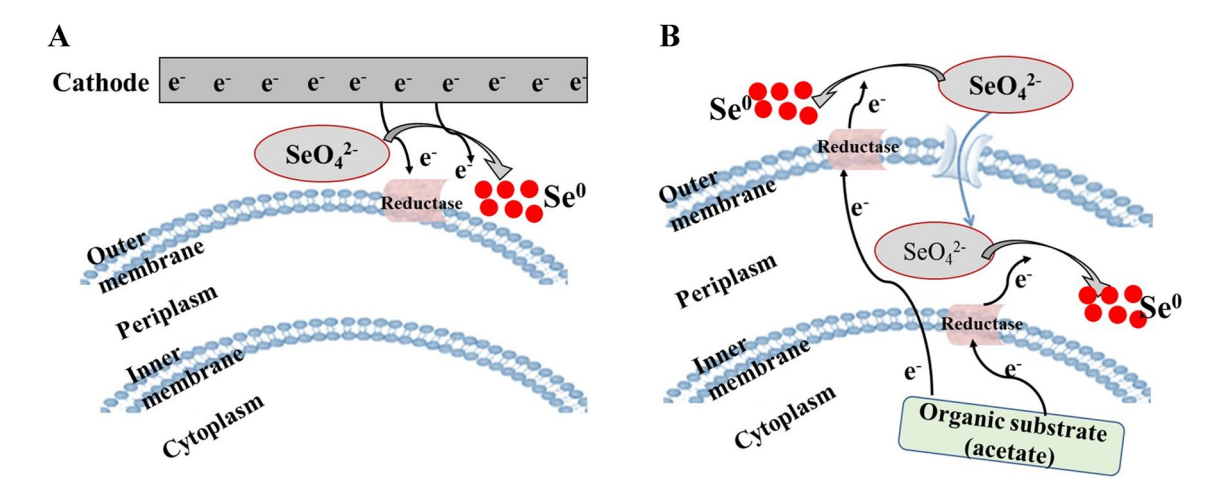


Fig. 6 Comparative schematic flow diagram representing the mechanisms of selenate reduction to elemental Se⁰ by enzymes of *Azospira* sp. A9D-23B A biocathode of BEC reactor: B conventional bioreactor

its roles in detoxification or respiration, similar to the *E. coli* cytoplasmic selenate reductase (Bébien et al. 2002).

Kinetics of selenate reduction

The maximum reaction rate corresponds to the enzyme completely saturated with the substrate. Using the linearized form of the Hans-Woolf equation, we applied linear regression to estimate the $K_{\rm m}$ and $V_{\rm max}$ parameters. In this linear representation, the slope corresponds to $1/V_{\text{max}}$, and the intercept corresponds to $K_{\text{m}}/V_{\text{max}}$. Extracting these parameters through the linear regression process facilitated the determination of $K_{\rm m}$ and $V_{\rm max}$. The resulting curves exhibited a high R^2 value (> 0.99), indicating a robust fit (Fig. S5). The lower the $K_{\rm m}$ value, the stronger the affinity of the enzyme to selenate. Interestingly, the $K_{\rm m}$ value was similar for the two cellular fractions of Azosipra A9D-23B in the two types of reactors (Table 1), suggesting that the different selenate reduction performance of Azosipra A9D-23B in the two types of reactors was not due to selenate affinity but due to the different specific enzyme activity discussed in the "Cellular location of selenate reductase in Azospira sp. A9D-23B" section. $K_{\rm m}$ of the active enzymes of Azospira sp. from the biocathode and conventional bioreactor were further compared with other selenate-reducing pure species from the literature (Table S1). Most of the species listed in Table S1 have larger K_m values compared to Azospira sp. in our study, which indicates that they have a lower affinity for selenate. The high specific activity for selenate reduction and a lower K_m value of the selenate reductase located in the outer and periplasmic fractions of strain A9D-23B indicated that the bacterium is more effective for the extracellular recovery of elemental Se⁰ when used in the BEC reactor.

Conclusions

The biosynthesis of elemental Se⁰ nanoparticles is an environmentally friendly process. This study demonstrates that the highly efficient selenate-reducing bacteria, Azospira sp. A9D-23B, uses different mechanisms to produce elemental Se⁰ in two distinct reactor configurations—a BEC reactor and a conventional bioreactor. Four major findings are presented in this study: (1) the ability of the bacteria in the reactors to remove the total dissolved selenium species (SeO₄²⁻, SeO₃²⁻, and Se²⁻) to levels below the USEPA standard, (2) the demonstration that the pure culture producing intracellular Se⁰ nanoparticles comprised less than 1% on the biocathode, but 35% in conventional bioreactor, (3) the location of the more active selenate reductases in the cells dictating the location of elemental Se⁰ production, and (4) the correlation of higher specific enzyme activity with lower cellular energy costs.

This study helps to understand the molecular processes underlying selenium recovery from Se-laden wastewater, offering a potential eco-friendly solution to selenium contamination. The results also provided novel and important insights into the kinetics and mechanisms of microbial selenium oxyanion reduction: the facultative anaerobic bacterium Azospira sp. A9D-23B can be used in BEC reactors to remove the contaminant below USEPA standards while also ensuring the exclusive recovery of elemental Se⁰. This work provides additional understanding of the regulation, selenate reduction mechanisms, and substrate preferences. The promising results of this sustainable and eco-friendly microbial approach indicated strong commercial viability for upscaling BEC reactors with Azospira sp. A9D-23B using real Se-laden wastewater. Given the increasing regulatory pressures to manage selenium contamination, this technology offers a viable solution



for industries to meet stringent environmental standards and ensure regulatory compliance. The potential for commercialization lies in its ability to provide an effective, cost-efficient, and environmentally sustainable method for selenium removal from wastewater.

Supplementary Information The online version contains supplementary material available at https://doi.org/10.1007/s11356-024-35140-6.

Acknowledgements The authors express their sincere gratitude to Dr. Yan Xin and Mr. Grayson Platt at Florida State University for their invaluable technical assistance in STEM and TEM imaging and to Cheryl Pye and Steve Miller at the DNA sequencing facility at Florida State University for 16S rRNA sequencing. TEM analyses were performed at Florida State University's Biological Science Imaging Resource using the Hitachi HT7800 instrument, supported by the NSF grant #2017869. The work conducted at the National High Magnetic Field Laboratory receives support from the NSF Division of Chemistry and Division of Materials Research through DMR-2128556, as well as the State of Florida. Cell lysis, separation of outer and periplasmic enzymes from the inner and cytoplasmic enzymes, and activity assay were performed at the Institute of Molecular Biophysics.

Author contribution BKA: conceptualization, investigation, methodology, formal analysis, and writing—original draft. NW: methodology, analysis, and writing—review and editing. MES: methodology and writing—review and editing. YT: conceptualization, methodology, formal analysis, funding acquisition, resources, supervision, and writing—review and editing. HC: conceptualization, methodology, formal analysis, funding acquisition, resources, supervision, and writing—review and editing.

Funding This research received funding from the National Science Foundation (NSF) through grant #2029682 awarded to Florida State University.

Data availability Data that support the findings of this study are available on request from the corresponding authors. The 16S rRNA partial sequence of *Azospira* sp. A9D-23B was deposited into Genbank under accession no. OO983537.

Declarations

Ethics approval and consent to participate Not applicable.

Consent for publication All authors agreed to publish the work.

Competing interests The authors declare no competing interests.

References

- Bébien M, Lagniel G, Garin J et al (2002) Involvement of superoxide dismutases in the response of Escherichia coli to selenium oxides. J Bacteriol. https://doi.org/10.1128/JB.184.6.1556-1564.2002
- Butler CS, Debieux CM, Dridge EJ, Splatt P, Wright M (2012) Biomineralization of selenium by the selenate-respiring bacterium Thauera selenatis. Biochem Soc Trans 40(6):1239–43. https://doi.org/10.1042/BST20120087
- Choi MJ, Chae KJ, Ajayi FF et al (2011) Effects of biofouling on ion transport through cation exchange membranes and microbial

- fuel cell performance. Bioresour Technol 102. https://doi.org/10.1016/j.biortech.2010.06.129
- Debieux CM, Dridge EJ, Mueller CM et al (2011) A bacterial process for selenium nanosphere assembly. Proc Natl Acad Sci U S A 108. https://doi.org/10.1073/pnas.1105959108
- Felsenstein J (1985) Confidence limits on phylogenies: an approach using the bootstrap. Evolution (n y). https://doi.org/10.2307/2408678
- Fernández-Llamosas H, Castro L, Blázquez ML et al (2017) Speeding up bioproduction of selenium nanoparticles by using Vibrio natriegens as microbial factory. Sci Rep. https://doi.org/10.1038/s41598-017-16252-1
- Fernández-Llamosas H, Castro L, Blázquez ML et al (2016) Biosynthesis of selenium nanoparticles by Azoarcus sp. CIB. Microb Cell Fact 15. https://doi.org/10.1186/s12934-016-0510-y
- Gingerich DB, Grol E, Mauter MS (2018) Fundamental challenges and engineering opportunities in flue gas desulfurization wastewater treatment at coal fired power plants. Environ Sci Water Res Technol 4. https://doi.org/10.1039/c8ew00264a
- Graedel TE, Harper EM, Nassar NT et al (2015) Criticality of metals and metalloids. Proc Natl Acad Sci U S A 112. https://doi.org/10.1073/pnas.1500415112
- Guymer D, Maillard J, Sargent F (2009) A genetic analysis of in vivo selenate reduction by Salmonella enterica serovar Typhimurium LT2 and Escherichia coli K12. Arch Microbiol. https://doi.org/10. 1007/s00203-009-0478-7
- Hatfield DL, Tsuji PA, Carlson BA, Gladyshev VN (2014) Selenium and selenocysteine: roles in cancer, health, and development. Trends Biochem Sci. https://doi.org/10.1016/j.tibs.2013.12.007
- Haygarth PM. (1994) Global importance and global cycling of selenium. In: Frankenberger WT, Benson Sally, editors. Selenium in the Environment.New York, USA: Marcel Dekker, p. 1–28
- Holmes AB, Ngan A, Giesinger K, Gu F (2023) Tunable production of elemental Se vs. H2Se through photocatalytic reduction of selenate in synthetic mine impacted brine: engineering a recoverable Se product. Environ Sci Water Res Technol. https://doi.org/10.1039/d2ew00553k
- Hunter WJ (2007) An Azospira oryzae (syn Dechlorosoma suillum) strain that reduces selenate and selenite to elemental red selenium. Curr Microbiol 54, https://doi.org/10.1007/s00284-006-0474-y
- Kashiwa M, Nishimoto S, Takahashi K et al (2000) Factors affecting soluble selenium removal by a selenate-reducing bacterium Bacillus sp. SF-1. J Biosci Bioeng 89. https://doi.org/10.1016/S1389-1723(00)80051-1
- Kessi J, Ramuz M, Wehrli E et al (1999) Reduction of selenite and detoxification of elemental selenium by the phototrophic bacterium Rhodospirillum rubrum. Appl Environ Microbiol 65. https:// doi.org/10.1128/aem.65.11.4734-4740.1999
- Krafft T, Bowen A, Theis F, MacY JM (2000) Cloning and sequencing of the genes encoding the periplasmic-cytochrome b-containing selenate reductase of Thauera selenatis. Mitochondrial DNA. https://doi.org/10.3109/10425170009015604
- Kuroda M, Yamashita M, Miwa E et al (2011) Molecular cloning and characterization of the srdBCA operon, encoding the respiratory selenate reductase complex, from the selenate-reducing bacterium Bacillus selenatarsenatis SF-1. J Bacteriol 193. https://doi.org/10.1128/JB.01197-10
- Lafontaine M, Lancaster CRD (2015) An unconventional anaerobic membrane protein production system based on Wolinella succinogenes. Methods Enzymol 556:99–121. https://doi.org/10.1016/ bs.mie.2014.12.026
- Lai CY, Wen LL, Shi LD et al (2016) Selenate and nitrate bioreductions using methane as the electron donor in a membrane biofilm reactor. Environ Sci Technol. https://doi.org/10.1021/acs.est.6b02807
- Lai CY, Song Y, Wu M et al (2020) Microbial selenate reduction in membrane biofilm reactors using ethane and propane as electron



- donors. Water Res 183. https://doi.org/10.1016/j.watres.2020. 116008
- Lampis S, Zonaro E, Bertolini C et al (2017) Selenite biotransformation and detoxification by Stenotrophomonas maltophilia SeITE02: novel clues on the route to bacterial biogenesis of selenium nanoparticles. J Hazard Mater 324. https://doi.org/10.1016/j.jhazmat. 2016.02.035
- Lenz M, Enright AM, O'Flaherty V et al (2009) Bioaugmentation of UASB reactors with immobilized Sulfurospirillum barnesii for simultaneous selenate and nitrate removal. Appl Microbiol Biotechnol. https://doi.org/10.1007/s00253-009-1915-x
- Li B, Liu N, Li Y et al (2014a) Reduction of selenite to red elemental selenium by Rhodopseudomonas palustris strain N. PLoS ONE. https://doi.org/10.1371/journal.pone.0095955
- Li DB, Cheng YY, Wu C et al (2014b) Selenite reduction by Shewanella oneidensis MR-1 is mediated by fumarate reductase in periplasm. Sci Rep 4. https://doi.org/10.1038/srep03735
- Liang X, Gadd GM (2017) Metal and metalloid biorecovery using fungi. Microb Biotechnol 10. https://doi.org/10.1111/1751-7915.12767
- Losi ME, Frankenberger WT (1997) Reduction of selenium oxyanions by Enterobacter cloacae SLD1a-1: isolation and growth of the bacterium and its expulsion of selenium particles. Appl Environ Microbiol. https://doi.org/10.1128/aem.63.8.3079-3084.1997
- Ma J, Kobayashi DY, Yee N (2007) Chemical kinetic and molecular genetic study of selenium oxyanion reduction by Enterobacter cloacae SLD1a-1. Environ Sci Technol. https://doi.org/10.1021/ es0712672
- Macy JM, Michel TA, Kirsch DG (1989) Selenate reduction by a Pseudomonas species: a new mode of anaerobic respiration. FEMS Microbiol Lett 61. https://doi.org/10.1111/j.1574-6968.1989.tb03577.x
- Macy JM, Lawson S, DeMoll-Decker H (1993a) Bioremediation of selenium oxyanions in San Joaquin drainage water using Thauera selenatis in a biological reactor system. Appl Microbiol Biotechnol 40. https://doi.org/10.1007/BF00175752
- Macy JM, Rech S, Auling G et al (1993b) Thauera selenatis gen. nov., sp. nov., a member of the beta subclass of Proteobacteria with a novel type of anaerobic respiration. Int J Syst Bacteriol 43. https:// doi.org/10.1099/00207713-43-1-135
- Moss RL, Tzimas E, Kara H, Willis P, Kooroshy J (2011) Critical Metals in Strategic Energy Technologies Assessing Rare Metals as Supply-Chain Bottlenecks in Low-Carbon Energy Technologies (EUR--24884-EN-2011). The Netherlands. https://setis.ec. europa.eu/system/files/2021-01/CriticalMetalsinStrategicEnerg yTechnologies-def.pdf. Accessed 10 March 2023
- Murray DT, Weiss KL, Stanley CB, Gergely Nagy MES (2021) Small-angle neutron scattering solution structures of NADPH-dependent sulfite reductase. J Struct Biol 213:107724. https://doi.org/10.1016/j.jsb.2019.01.001
- Nancharaiah Y V., Lens PNL (2015) Selenium biomineralization for biotechnological applications. Trends Biotechnol 33. https://doi. org/10.1016/j.tibtech.2015.03.004
- Negi BB, Sinharoy A, Pakshirajan K (2020) Selenite removal from wastewater using fungal pelleted airlift bioreactor. Environ Sci Pollut Res 27. https://doi.org/10.1007/s11356-019-06946-6
- Nguyen VK, Park Y, Yu J, Lee T (2016) Microbial selenite reduction with organic carbon and electrode as sole electron donor by a bacterium isolated from domestic wastewater. Bioresour Technol. https://doi.org/10.1016/j.biortech.2016.04.033
- Nguyen VK, Nguyen TH, Ha MG, Kang HY (2019) Kinetics of microbial selenite reduction by novel bacteria isolated from activated sludge. J Environ Manage. https://doi.org/10.1016/j.jenvman. 2019.02.012
- Oremland RS, Blum JS, Bindi AB et al (1999) Simultaneous reduction of nitrate and selenate by cell suspensions of selenium-respiring

- bacteria. Appl Environ Microbiol 65. https://doi.org/10.1128/aem. 65.10.4385-4392.1999
- Oremland RS, Herbel MJ, Blum JS et al (2004) Structural and spectral features of selenium nanospheres produced by Se-respiring bacteria. Appl Environ Microbiol 70. https://doi.org/10.1128/AEM. 70.1.52-60.2004
- Osborn MJ, Munson R (1974) [67] Separation of the inner (cytoplasmic) and outer membranes of gram-negative bacteria. Methods Enzymol. https://doi.org/10.1016/0076-6879(74)31070-1
- Pearce CI, Pattrick RAD, Law N et al (2009) Investigating different mechanisms for biogenic selenite transformations: Geobacter sulfurreducens, Shewanella oneidensis and Veillonella atypica. Environ Technol 30. https://doi.org/10.1080/09593330902984751
- Prakash NT, Sharma N, Prakash R et al (2009) Aerobic microbial manufacture of nanoscale selenium: exploiting nature's bionanomineralization potential. Biotechnol Lett. https://doi.org/10.1007/s10529-009-0096-0
- Rayman MP (2002) Se brought to Earth. Chem Br 38:28-31
- Ridley H, Watts CA, Richardson DJ, Butler CS (2006) Resolution of distinct membrane-bound enzymes from Enterobacter cloacae SLD1a-1 that are responsible for selective reduction of nitrate and selenate oxyanions. Appl Environ Microbiol. https://doi.org/ 10.1128/AEM.00568-06
- Saitou N, Nei M (1987) The neighbor-joining method: a new method for reconstructing phylogenetic trees. Mol Biol Evol. https://doi. org/10.1093/oxfordjournals.molbev.a040454
- Schröder I, Rech S, Krafft T, Macy JM (1997) Purification and characterization of the selenate reductase from Thauera selenatis. J Biol Chem. https://doi.org/10.1074/jbc.272.38.23765
- Shakibaie M, Khorramizadeh MR, Faramarzi MA et al (2010) Biosynthesis and recovery of selenium nanoparticles and the effects on matrix metalloproteinase-2 expression. Biotechnol Appl Biochem 56. https://doi.org/10.1042/ba20100042
- Sinharoy A, Lens PNL (2022) Selenite and tellurite reduction by Aspergillus niger fungal pellets using lignocellulosic hydrolysate. J Hazard Mater. https://doi.org/10.1016/j.jhazmat.2022.129333
- Soda S, Kashiwa M, Kagami T et al (2011) Laboratory-scale bioreactors for soluble selenium removal from selenium refinery wastewater using anaerobic sludge. Desalination 279. https://doi.org/10.1016/j.desal.2011.06.031
- Sonkusre P, Nanduri R, Gupta P, Cameotra SS (2014) Improved extraction of intracellular biogenic selenium nanoparticles and their specificity for cancer chemoprevention. J Nanomedicine Nanotechnol 5. https://doi.org/10.4172/2157-7439.1000194
- Stadtman TC (1996) Selenocysteine. Annu Rev. Biotechnol 65:83–100. https://doi.org/10.1146/annurev.bi.65.070196.000503
- Staicu LC, van Hullebusch ED, Lens PNL (2015) Production, recovery and reuse of biogenic elemental selenium. Environ Chem Lett 13:80_06
- Stolz JF, Oremland RS (1999) Bacterial respiration of arsenic and selenium. FEMS Microbiol. Rev 23. https://doi.org/10.1111/j.1574-6976.1999.tb00416.x
- Switzer Blum J, Stolz JF, Oren A, Oremland RS (2001) Selenihalanaerobacter shriftii gen. nov., sp. nov., a halophilic anaerobe from Dead Sea sediments that respires selenate. Arch Microbiol 175. https://doi.org/10.1007/s002030100257
- Tamura K, Nei M, Kumar S (2004) Prospects for inferring very large phylogenies by using the neighbor-joining method. Proc Natl Acad Sci U S A. https://doi.org/10.1073/pnas.0404206101
- Tamura K, Stecher G, Kumar S (2021) MEGA11: Molecular Evolutionary Genetics Analysis Version 11. Mol Biol Evol. https://doi.org/10.1093/molbev/msab120
- Tan LC, Nancharaiah YV, Van Hullebusch ED, Lens PNL (2018a) Effect of elevated nitrate and sulfate concentrations on selenate removal by mesophilic anaerobic granular sludge bed reactors.



- Environ Sci Water Res Technol. https://doi.org/10.1039/c7ew0 0307b
- Tan Y, Wang Y, Wang Y et al (2018b) Novel mechanisms of selenate and selenite reduction in the obligate aerobic bacterium Comamonas testosteroni S44. J Hazard Mater. https://doi.org/10.1016/j. jhazmat.2018.07.014
- Tan Y, Yao R, Wang R et al (2016) Reduction of selenite to Se(0) nanoparticles by filamentous bacterium Streptomyces sp. ES2–5 isolated from a selenium mining soil. Microb Cell Fact. https://doi.org/10.1186/s12934-016-0554-z
- Tang Y, Chen G (2019) Reactors and methods for producing and recovering extracellular metal or metalloid nanoparticles. US Pat 11(008):234
- Tang Y, Werth CJ, Sanford RA et al (2015) Immobilization of selenite via two parallel pathways during in situ bioremediation. Environ Sci Technol 49. https://doi.org/10.1021/es506107r
- Theisen J, Yee N (2014) The molecular basis for selenate reduction in Citrobacter freundii. Geomicrobiol J. https://doi.org/10.1080/01490451.2014.907377
- USEPA (2015) Drinking water contaminants: National Primary Drinking Water Regulations. US EPA website https://water.epa.gov/drink/contaminants/index.cfm. Accessed 12 Jan 2023
- USEPA (2019) Title 40-Chapter 1-CFR Part 423, Effluent Limitations Guidelines and Standards for the Steam Electric Power Generating Point Source Category. In: Fed. Regist. vol. 85, no. 198. https://www.federalregister.gov/documents/2019/11/22/2019-24686/effluent-limitations-guidelines-and-standards-for-the-steam-electric-power-generating-point-source. Accessed 12 Jan 2023
- Vazquez A, Beg QK, deMenezes MA et al (2008) Impact of the solvent capacity constraint on E. coli metabolism. BMC Syst Biol. https:// doi.org/10.1186/1752-0509-2-7
- Wang Y, Shu X, Zhou Q et al (2018) Selenite reduction and the biogenesis of selenium nanoparticles by Alcaligenes faecalis se03 isolated from the gut of Monochamus alternatus (Coleoptera: Cerambycidae). Int J Mol Sci. https://doi.org/10.3390/ijms19092799
- Watts CA, Ridley H, Condie KL et al (2003) Selenate reduction by Enterobacter cloacae SLD1a-1 is catalysed by a

- molybdenum-dependent membrane-bound enzyme that is distinct from the membrane-bound nitrate reductase. FEMS Microbiol Lett. https://doi.org/10.1016/S0378-1097(03)00782-1
- Xu D, Yang L, Wang Y et al (2018) Proteins enriched in charged amino acids control the formation and stabilization of selenium nanoparticles in Comamonas testosteroni S44. Sci Rep. https://doi.org/10. 1038/s41598-018-23295-5
- Yee N, Ma J, Dalia A et al (2007) Se(VI) reduction and the precipitation of Se(0) by the facultative bacterium Enterobacter cloacae SLD1a-1 are regulated by FNR. Appl Environ Microbiol. https:// doi.org/10.1128/AEM.02542-06
- Zhang Z, Xiong Y, Chen H, Tang Y (2020) Understanding the composition and spatial distribution of biological selenate reduction products for potential selenium recovery. Environ Sci Water Res Technol. https://doi.org/10.1039/d0ew00376j
- Zhang Z, Asefaw BK, Xiong Y et al (2022) Evidence and mechanisms of selenate reduction to extracellular elemental selenium nanoparticles on the biocathode. Environ Sci Technol 56:16259–16270. https://doi.org/10.1021/acs.est.2c05145
- Zhang Z, Adedeji I, Chen G, Tang Y (2018a) Chemical-free recovery of elemental selenium from selenate-contaminated water by a system combining a biolog ical reactor, a bacterium-nanoparticle separator, and a tangential flow filter. Environ Sci Technol 52. https://doi.org/10.1021/acs.est.8b04544
- Zhang Z, Chen G, Tang Y (2018b) Towards selenium recovery: biocathode induced selenate reduction to extracellular elemental selenium nanoparticles. Chem Eng J 351. https://doi.org/10.1016/j. cej.2018.06.172

Publisher's Note Springer Nature remains neutral with regard to jurisdictional claims in published maps and institutional affiliations.

Springer Nature or its licensor (e.g. a society or other partner) holds exclusive rights to this article under a publishing agreement with the author(s) or other rightsholder(s); author self-archiving of the accepted manuscript version of this article is solely governed by the terms of such publishing agreement and applicable law.

Authors and Affiliations

Benhur Kessete Asefaw¹ · Nidhi Walia^{2,3} · Margaret Elizabeth Stroupe^{2,3} · Huan Chen⁴ · Youneng Tang¹

- ☐ Huan Chen huan.chen@magnet.fsu.edu
- Department of Civil and Environmental Engineering, FAMU-FSU College of Engineering, Florida State University, 2525 Pottsdamer Street, Tallahassee, FL 32310, USA
- Department of Biological Science, Florida State University, 91 Chieftain Way, Tallahassee, FL 32306, USA
- Institute of Molecular Biophysics, Florida State University, 91 Chieftain Way, Tallahassee, FL 32306, USA
- ⁴ National High Magnetic Field Laboratory, Florida State University, 1800 East Paul Dirac Drive, Tallahassee, FL 32310, USA

